DD

STATE RESEARCH CENTER OF RUSSIA

INSTITUTE FOR HIGH ENERGY PHYSICS

IHEP 95-109

Yu.M.Goncharenko, O.A.Grachov, V.F.Kurshetsov,
L.G.Landsberg, S.B.Nurushev, A.N.Vasiliev

PHOTON DETECTOR FOR HIGH ENERGY MEASUREMENTS IN THE SELEX SPECTROMETER (FERMILAB EXPERIMENT E781)

Protvino 1995

UDK 681.3.06.069 M–24

Abstract

Goncharenko Yu.M. et al. Photon Detector for High Energy Measurements in the Selex Spectrometer (Fermilab Experiment E781): IHEP Preprint 95-109. – Protvino, 1995. – p. 22, figs. 17, tables 4, refs.: 11.

A possibility to use one or two photon lead glass detectors for high energy measurements in the SELEX spectrometer (with E_γ up to 500 GeV) is studied. It is concluded that it is possible to use a single photon detector, equipped with radiative resistant lead glass counters. For the best energy resolution in the case of Primakoff effect like $\pi^- + \gamma^* \to \pi^- + \gamma$ the combined method would be used with weighted combination of direct E_γ measurement in the Photon-3 detector and the beam constraint method.

Аннотация

Гончаренко Ю.М. и др. Фотонный детектор для измерений при высоких энергиях для спектрометра SELEX (эксперимент E781, Fermilab): Препринт ИФВЭ 95-109. – Протвино, 1995. – 22 с., 17 рис., 4 табл., библиогр.: 11.

Рассмотрена возможность использования в составе спектрометра SELEX одного или двух детекторов из свинцового стекла для измерений высокоэнергичных γ-квантов (вплоть до энергий 500 ГэВ). Сделан вывод о том, что возможно использование одного детектора, оборудованного счетчиками из радиационно-стойкого стекла. Для получения наилучшего энергетического разрешения для процессов типа эффекта Примакова $\pi^- + \gamma^* \to \pi^- + \gamma$ может применяться комбинированный метод, использующий взвешанное прямое измерение энергии γ-квантов в детекторе PHOTON-3 и точное измерение энергии пучка π^--мезонов.

1. Introduction

One of the main requirements for successful experiments in modern hadron spectroscopy (at nb level) is a possibility to detect not only charged secondaries, but neutral ones as well, i.e. photons from the radiative decays of secondary hadrons ($\pi^o \rightarrow \gamma\gamma$, $\eta \rightarrow \gamma\gamma$, $\Sigma^o \rightarrow \Lambda\gamma$ etc.). Particular attention has been given to the radiative decays of hadrons under study, for example, $\Xi_c^* \rightarrow \Xi_c + \gamma$ and so on.

The photon detection system of the SELEX spectrometer used in the experiment E781 Fermilab is an essential part of equipment [1,2]. It will be used in different branches of the experimental program – in the study of charmed physics, electromagnetic formfactors of hyperons, Primakoff effects, i.e. processes in the Coulomb field of nuclei (measurements of pions polarizability and radiative widths of hadrons, search for exotic mesons), in the search for charmed Pentaquark baryons and cryptoexotic strange baryons with additional hidden strangeness, etc.

The layout of the SELEX setup is presented in Fig.1. In order to obtain the large angular acceptance for photons (up to 100 mrad) and not to kill the charged secondaries, the photon detection system of E781 is split in 3 independent detectors schematically shown in Figs. 1 and 2

Photon-1 – in front of the magnet M2;	}	with the holes for charged particles to come through the aperture of the magnets.
Photon-2 – in front of the magnet M3;		
Photon-3 – in the rear of the magnet M3		

For the experiment on charmed baryons spectroscopy the energy range of these photon detectors are:

for Photon 1 –	$1 < E_\gamma < 20\ GeV$;	$\langle E_\gamma \rangle \simeq 4.5\ GeV$;
for Photon 2 –	$1 < E_\gamma < 50\ GeV$;	$\langle E_\gamma \rangle \simeq 15\ GeV$;
for Photon 3 –	$5 < E_\gamma < 100\ GeV$;	$\langle E_\gamma \rangle \simeq 35 - 40\ GeV$.

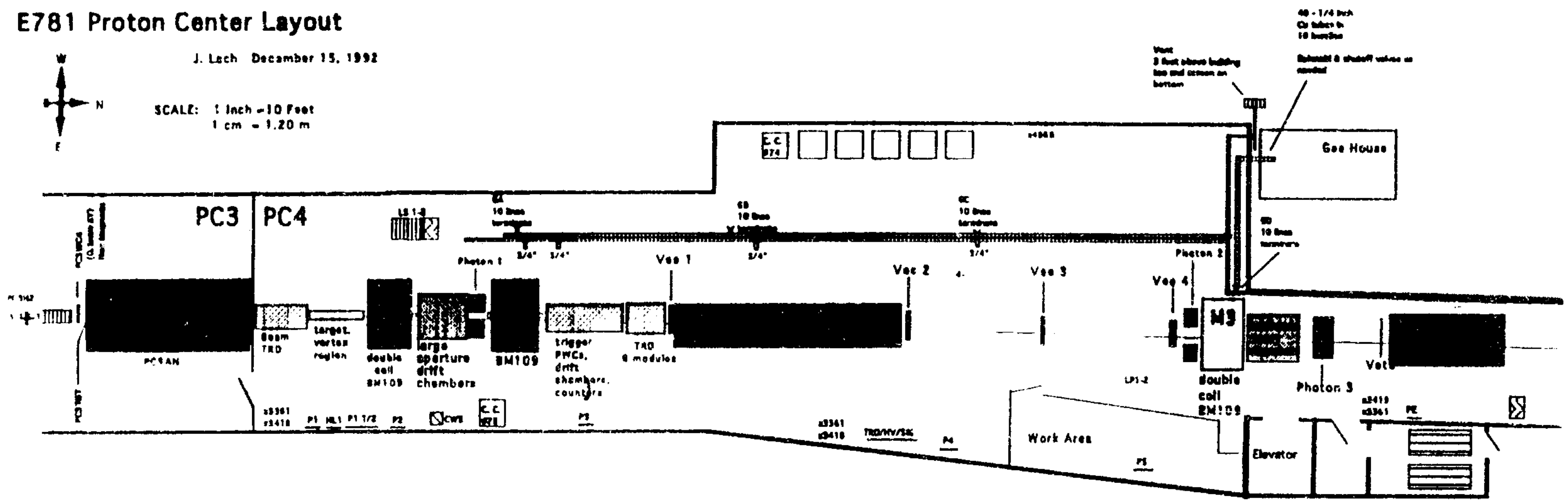

Fig. 1.

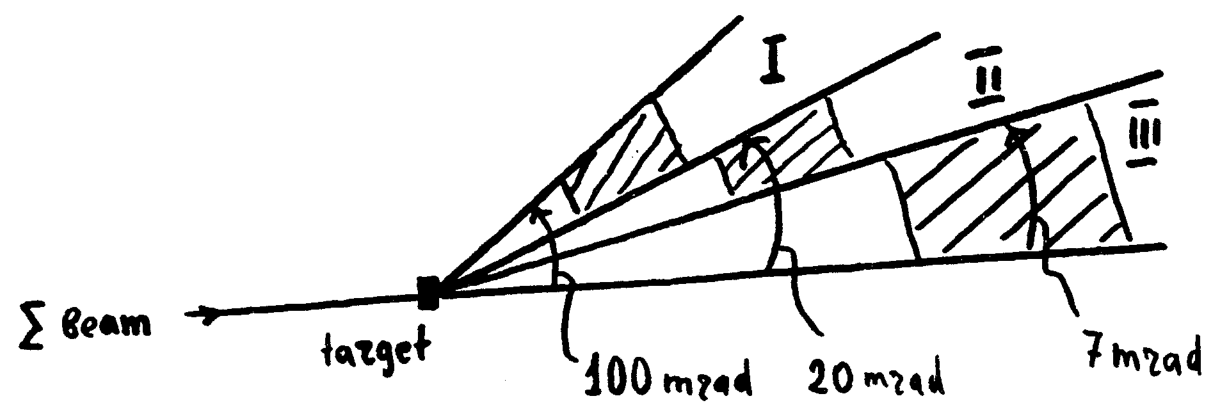

Fig. 2. Scheme of the Photon-1 – Photon-3 arrangement in the SELEX facility.

But for the measurements of pion polarizability in the Coulomb field production reaction $\pi^- + Pb \rightarrow \pi^- + \gamma + Pb$ the operating range of the Photon-3 detector would be extended up to $E_\gamma \simeq 500$ GeV. Thus the dynamical range for the Photon-3 spectrometer has to be quite large.

For the construction of the Photon-3 detector of E781 the elements of IHEP lead glass spectrometers from E704 [3] will be used. The Photon-3 detector is the matrix of 21×16 counters from TF1 or partly from radiative resistant lead glass TF101 with the dimensions of $3.82 \times 3.82 \times 45.0$ cm^3 for each block (for more details see Appendix 1). But the total thickness of the available lead glass (~16-18 radiative lengths) is not enough to work with E_γ of several hundreds GeV with maximal energy resolution because of substantial energy leakage (of the order of 10-20% in these electromagnetic showers).

To avoid this difficulty it was proposed to use two identical detectors – the Photon-3 and the Photon-4, which must be arranged one after another (Fig.3).

The preliminary study of energy resolution of the Photon-3 – Photon-4 system was performed in two H-notes by Z.H.Zhu [4]. It was found that the Photon-4 essentially improved the energy resolution of the system for high energy Primakoff photons in comparison with the Photon-3 alone. Unfortunately the geometry of the Photon-3 – Photon-4 system used in this calculations was not adequate to the real geometry of installation. The distance between the end of lead glass blocks of the Photon-3 and the beginning of lead glass blocks of the Photon-4 was assumed to be 105 cm, instead of the existing one of 150 cm. The greater distance between calorimeters diminishes the amount of energy reaching the Photon-4 and may cause the degradation of resolution. There are also exist many other factors that can affect the resolution and which were not taken into consideration in the simplified calculations of Z.H.Zhu. Among them are

1. Passive matter between Photons, consisting of photomultipliers, magnetic shieldings, bases, cables, plates, connectors, etc;
2. Beam hole in the Photon-4;
3. Finite energy threshold of the Photon-4;
4. Physical background due to the secondary interactions of accompaning Primakoff pion in photon detectors.

All these factors work in the same direction, diminishing the amount of measureable energy in the Photon-4 and may result in further degradation of the resolution. These were the reasons which forced us to recalculate the energy resolution of the Photon-3 – Photon-4 system in more realistic conditions.

2. Geometry of the Photon-3 - Photon-4 system

As it was said in Introduction, the geometry and construction of photon detectors are presented in Fig.3. Each photon detector consists of 21×16 lead glass counters with the dimensions of $3.82 \times 3.82 \times 45$ cm^3 and has a beam hole of 2×4 counters (in vertical $\times$ horizontal planes). The support frame installed in the beam hole is described in detail in Appendix 2. Just in front of the blocks there is an aluminum plate 1 cm thick.

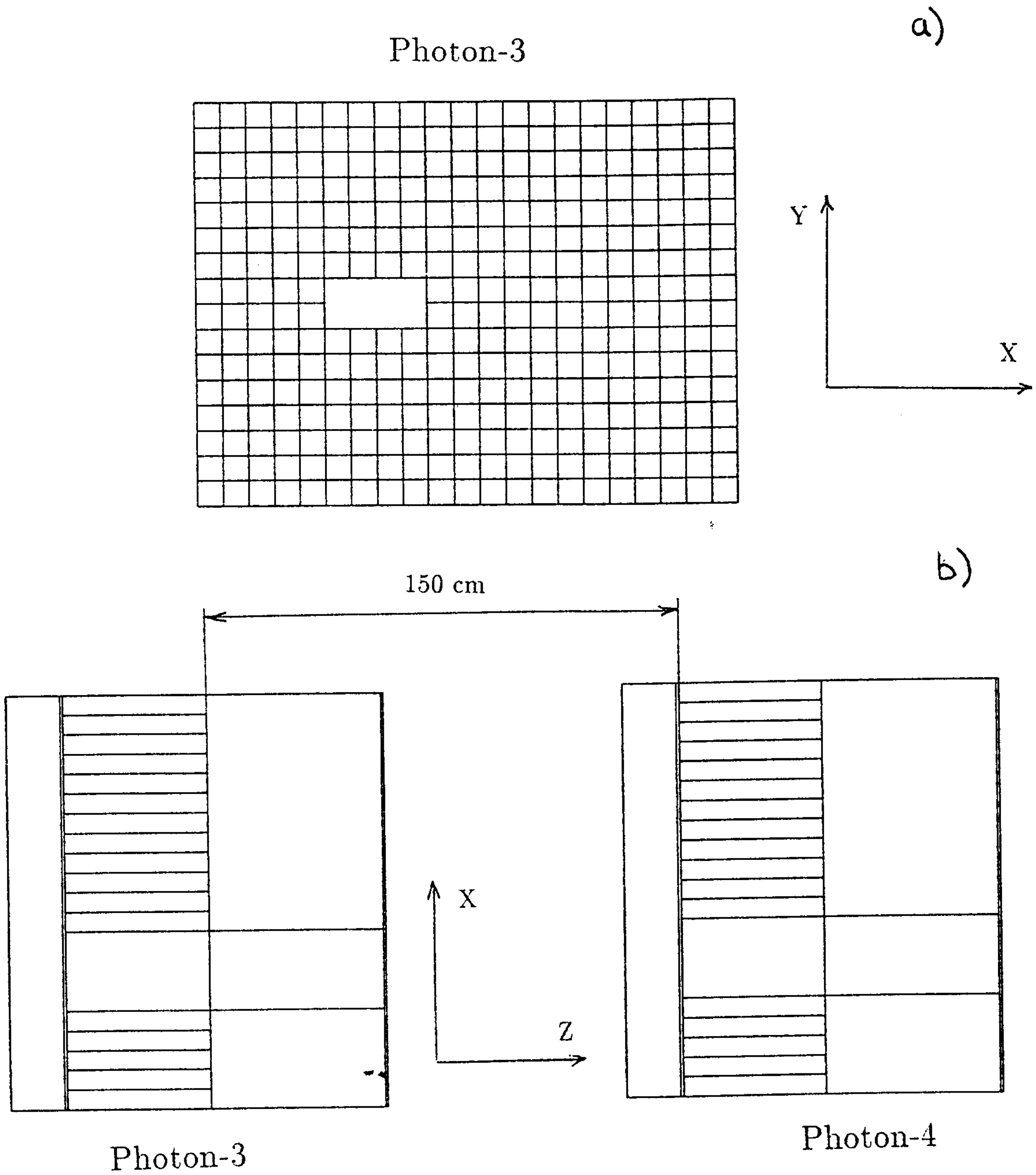

Fig. 3. The Photon-3 structure and the proposed arrangement of the Photon-3 and Photon-4 detectors: a) looking downstream; b) beam along Z axis.

The passive material after blocks was described as a homogenious medium with the properties of aluminum, but with the density 20% of it. This corresponds to 1.2 of radiation length in total. Each photon detector ends with the door made of aluminum plate 0.8 cm thick.

Most of calculations was made for the lead glass with the same parameters as in the previous calculations (R.L. = 2.36 cm, ρ = 3.86 g/cm^3, index of refraction = 1.67). In order to have a feeling about the influence of the value of radiation length of the glass we also about, on made some calculations for the glass with R.L. = 2.8 cm. We also assumed the same mean attenuation length of 80 cm for Cherenkov light inside the lead glass. The beam of γ's with fixed energy hit the Photon-3 exactly in the centre of detector. We used the GE781 Monte-Carlo code specially adapted for this task.

3. Energy leakage from the Photon-3

As the first step we calculated the energy leakage of electromagnetic showers from the Photon-3. This leakage can't depend on geometry (with the exception of the presence of the hole) and may be used to check the validity of the code and for the comparison of calculations with the experimental data at lower energies [4,5] and with the empirical approximation (curves 1 and 2 on Fig.4) based on EGS Monte-Carlo [6]

$$E_{\text{leak}}/E_{\text{in}} = 2.0\exp(-0.3X)E_{\text{in}}^{0.4}, \qquad (1)$$

where X is the thickness of the detector in the units of radiation length; E_{in} - the initial photon energy in GeV. The main results of our calculations with GE781 code were obtained with the energy cut for photon and electron energies equal to 1 MeV. The results of these calculations are shown in Fig.4 together with the experimental result of D0 test run at E_e = 100 GeV [5]. The D0 data, GAMS data (at E_e < 50 GeV) and our Monte-Carlo data at E_e = 30 GeV are in a good agreement with the results based on approximation (1). But at higher energies there is some systematic discrepancy between our Monte-Carlo calculations (solid line) and approximation (1) (Fig.4). In order to find the origin of this discrepancy we repeated the calculations for the energy of 100 GeV using lower threshold of 0.4 MeV and recieved much better agreement. Nevertheless we used the threshold of 1 MeV for the following reasons:

1. The natural threshold for Cherenkov radiation in lead glass is 0.64 MeV and up to 1 MeV the yield of Cherenkov photons is rather low;

2. γ's and electrons with the energy lower than 1 MeV have practically no chance to pass through the dead matter after the Photon-3 and hit the Photon-4;

3. The calculations with the threshold of 1 MeV are relatively time consuming (the simulation of one event with the initial energy of 500 GeV takes approximately 1 minute of CPU on SiG-computer in Fermilab).

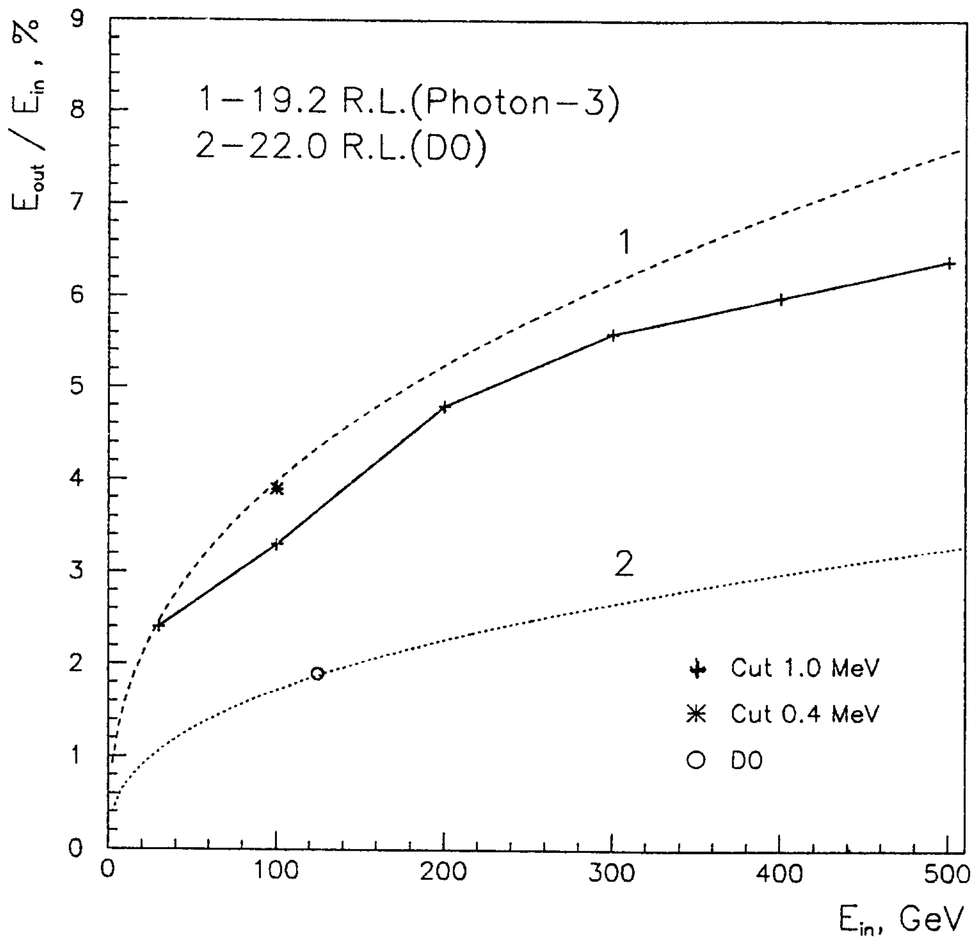

Fig. 4. Energy leakage from the rear part of the Photon-3 detector. Results of EGS Monte-Carlo approximation (see expression (1) in the text): curve 1 – for the detector thickness 19.2 r.l. (Photon-3); curve 2 – for 22 r.l. (D0); O – experimental data from D0 [5]; calculational with GE781 Monte-Carlo code with cut 1.0 MeV is presented by solid line (+); similar calculation with cut 0.4 MeV is pesented by *.

4. Measurable energy in the Photon-4

We calculated the energy resolution in the Photon-3 - Photon-4 system at six fixed energies: 10, 30, 100, 200, 300, 400 and 500 GeV. We assume the energy threshold for the individual counters in photon detectors to be 30 MeV. This is a very optimistic value, as compared with the practically used thresholds in the exeperiments with lead-glass photon detectors (50-60 MeV for GAMS, 100 MeV for SPHINX and E704, etc.).

↓ π^- ↓ γ

Photon 3

0	0	0	0	0	0	0	0	0	0	0	0	0	0	0	0	0	0	0	0	0
0	0	0	0	0	0	0	0	0	0	0	0	0	0	0	0	0	0	0	0	0
0	0	0	0	0	0	0	0	0	0	0	0	0	0	0	0	0	0	0	0	0
0	0	0	0	0	0	0	0	0	0	0	0	0	0	0	0	0	0	0	0	0
0	0	0	0	0	0	0	0	0	0	0	0	0	0	0	0	0	0	0	0	0
0	0	0	0	0	0	0	0	0	0	0	0	0	0	0	0	0	0	0	0	0
0	1	1	0	0	0	0	0	0	0	0	3	10	3	0	0	0	0	0	0	0
1	32	4	0	0					0	0	9	403	12	0	0	0	0	0	0	0
1	1	0	0	0					0	0	2	10	3	0	0	0	0	0	0	0
0	0	0	0	0	0	0	0	0	0	0	0	0	0	0	0	0	0	0	0	0
0	0	0	0	0	0	0	0	0	0	0	0	0	0	0	0	0	0	0	0	0
0	0	0	0	0	0	0	0	0	0	0	0	0	0	0	0	0	0	0	0	0
0	0	0	0	0	0	0	0	0	0	0	0	0	0	0	0	0	0	0	0	0
0	0	0	0	0	0	0	0	0	0	0	0	0	0	0	0	0	0	0	0	0
0	0	0	0	0	0	0	0	0	0	0	0	0	0	0	0	0	0	0	0	0
0	0	0	0	0	0	0	0	0	0	0	0	0	0	0	0	0	0	0	0	0

Photon 4

32	23	7	32	9	10	931	523	92	30	25	2	12	0	19	5	69	24	7	26	0
28	5	0	9	6	1	51	125	92	18	63	24	36	59	18	82	16	0	0	11	0
25	0	12	2	12	2	11	1960	441	9	42	5	28	25	55	29	20	110	19	4	0
4	18	23	0	0	14	11	948	2218	37	449	47	58	5	16	0	0	1	0	2	4
8	33	39	15	8	0	79	112	88	39	134	38	83	56	58	7	7	37	0	39	18
44	22	6	7	20	13	63	49	37	156	113	156	211	460	224	38	60	31	5	9	26
8	248	68	9	162	4	9	51	42	168	185	375	627	173	254	57	80	66	7	0	26
127	453	77	41	52					22	93	421	1161	772	363	90	12	6	18	23	6
54	70	709	48	49					65	96	462	603	190	73	61	120	45	18	99	25
55	54	242	30	18	28	20	23	295	223	441	63	578	75	40	22	34	23	9	0	82
44	84	1692	273	163	22	6	1	18	44	83	17	77	27	22	44	9	43	3	45	2
53	19	645	60	15	36	29	56	12	38	5	62	201	297	445	25	11	65	5	36	31
17	0	18	18	13	15	29	6	59	8	71	10	3	16	29	30	21	0	0	7	14
0	7	6	28	0	0	5	35	54	43	32	0	46	15	13	25	45	8	0	30	19
0	5	19	0	6	4	0	0	16	46	40	4	8	15	0	1	6	0	14	0	0
1	5	17	2	2	0	0	4	6	5	11	2	37	10	0	4	9	19	18	0	2

Fig. 5. Response of the Photon-3 – Photon-4 system to the typical Primakoff event $\pi^- + Pb \rightarrow \pi^- + \gamma + Pb$ with the secondaries with energies E_π=170 GeV and E_γ=480 GeV. The numbers in the Photon-3 are energies in GeV. The numbers in the Photon-4 are energies in MeV.

We also introduced the geometrical cut for the energy in the Photon-4. The necessity of such a cut can be clearly seen from Fig. 5, where the response of the Photon-3 - Photon-4 detectors to the typical Primakoff event is shown. The final state in this event consists of a charged pion with the energy of 170 GeV and a γ with the energy of 480 GeV. It is evident from the picture, that the pion interacting in the Photon-3 (70% of interaction length), gives very complicated pattern in the Photon-4 and the bumps of energy (comparable in the energy with a Primakoff photon) are distributed throughout the whole Photon-4 detector. The simplest and the only practical way to isolate the energy from γ is to introduce the geometrical cut defined as the area of 5 * 5 or 3 * 3 counters near the central counter, predicted from the pattern in the Photon-3. We must emphasize that the lower the energy of γ, the worse the situation is: the distance between pion and γ is smaller and the relative energy of pion in the Photon-4 is greater. In the calculations of the energy resolution we didn't use the real Primakoff events and simply introduce the geometrical cuts, so the the results of the calculations must be considered as optimistic.

5. Results for energy resolution

The results of our calculations are shown in Fig.6.

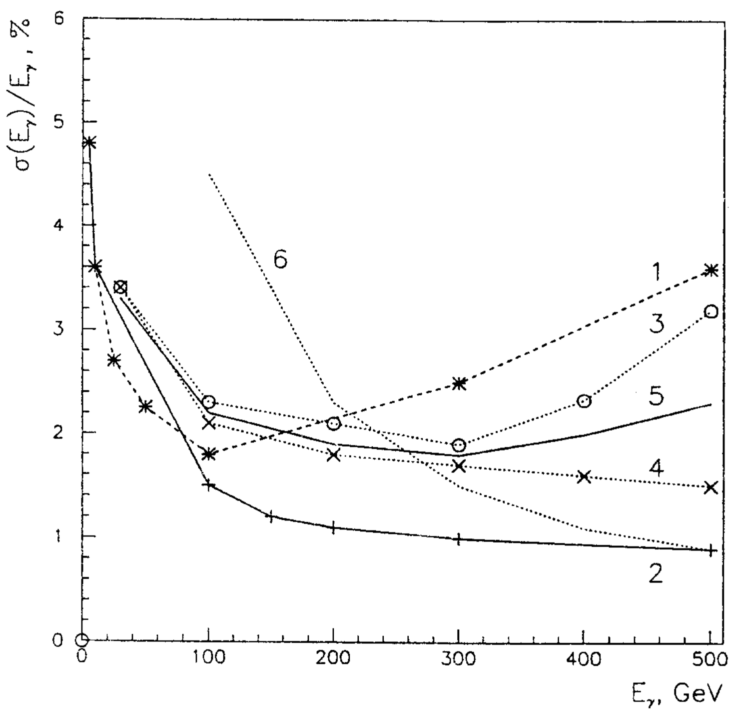

Fig. 6. Results of the calculation of energy resolution for the Photon-3 and the Photon-3 – Photon-4 system (for the thickness of detector 19 r.l.): 1 – old calculation [4] for the Photon-3 alone; 2 – old calculation [4] for the Photon-3 – Photon-4; 3 – present calculation for the Photon-3 alone; 4 – present calculation for the Photon-3 – Photon-4 with the assumption that the whole energy in the Photon-4 can be measured; 5 – present calculation for the Photon-3 – Photon-4 system under real conditions (with all the cuts described in the text); 6 – resolution for the beam constrained method of E_γ measurement in the reaction $\pi^- + Pb \to \pi^- + \gamma + Pb$.

The curve 6 in Fig.6 corresponds to the assumption that the resolution for the primary pion beam is 0.7% and the energy of γ can be calculated as $E_\gamma = E_{beam} - E_{\pi^-}$ (E_{π^-} the energy of secondary pion). It is seen from this curves, that our result for the "ideal" Photon-3 – Photon-4 system is by a factor of 1.6-1.7 worse than that of [4]. This is mainly due to the greater distance between photons in the present geometry. It is also seen that for the "realistic" Photon-3 – Photon-4 system the energy resolution for the energy of 500 GeV is worse by another factor of 1.5. We can conclude from this figure that:

1. The resolution of the Photon-3 – Photon-4 system will be approximately constant (above 100 GeV) and equal to $2 - 2.5\%$.

2. The Photon-4 only slightly improves the energy resolution as compared to the Photon-3 alone.

3. For Primakoff-type experiments it seems that the best way is to use only the Photon-3 detector with a combined method of energy determination for γ-rays: the weighted measurements of E_γ from the Photon-3 data (direct measurement) and from the beam constraint procedure (indirect method) (Fig.7). Practically for $E_\gamma \leq 200$ GeV the main results would be obtained by the direct method and for higher energy – by the beam constraint procedure. In the last case the Photon-3 is only used to measure impact point of γ. The expected precision in the coordinate measurements at $E_\gamma \simeq 400$ GeV is $\sigma_{x,y} \simeq 0.7 - 0.8$ mm.

We also calculated the energy resolution of photon detectors for the 500 GeV energy of γ using smaller value of radiation length of lead glass: (R.L. = 2.8 cm), because of some uncertainty in the existing data on the radiative length for our lead glass counters. The point is that in this case the energy leakage from the Photon-3 is greater and it may turn out that the Photon-4 is more useful. In reality we received the energy resolution of the Photon-3 being 6% and for the combined system – $3.3 - 3.8\%$. We also calculated the realistic energy resolution for the 105 cm distance between two photon detectors (as in [3] and found the resolution to be about $1.5 - 1.8\%$ for 500 Gev γ's. This is also worse than in the indirect measurement from beam constraint. Thus, in any case the best results for the energy resolution would be obtained for the single Photon-3 detector with combined Photon-3/(beam constraint) method.

It seems desirable to use an additional lead converter before the Photon-3 with the thickness of 1.5 rad.length. Such a converter will improve the energy resolution for moderate energy photons, where the indirect measurements from beam constraint are not accurate. At the same time this passive converter will not distort the resolution of γ - detector even for low energy photons. This was stated in the special measurements with such a converter in BNL experiment [7]. The results of these measurements are presented in Table 1.

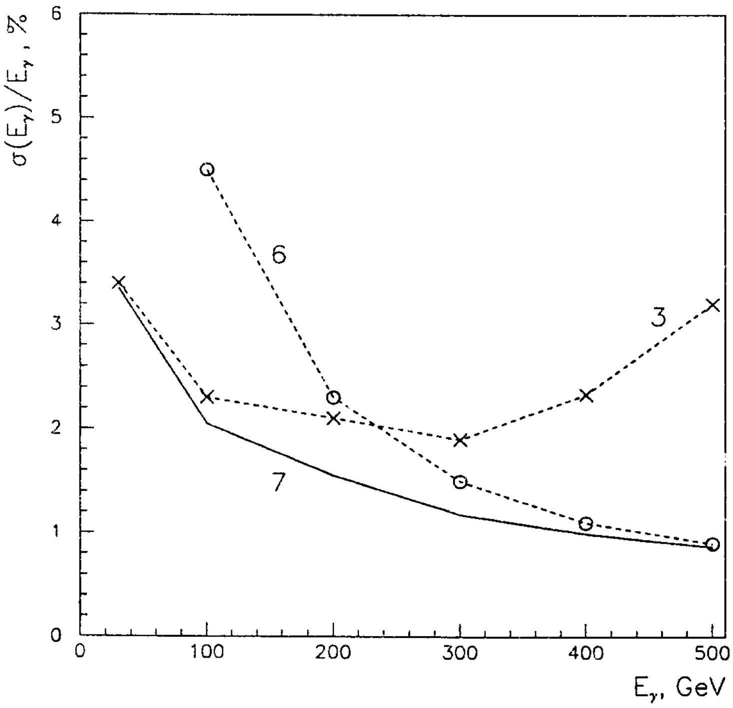

Fig. 7. Expected resolution for the combined method of the photon energy measurement in the reaction $\pi^- + Pb \rightarrow \pi^- + \gamma + Pb$ (the weighted average of the direct mesurement in the Photon-3 detector and indirect evaluation by the beam constrained method): 3,6 – the same as in Fig.6; 7 – weighted average of the curves 3 and 6.

Table 1. Effect of pre-radiator on energy resolution

Beam Energy(GeV)	Pre-radiator Thickness (Rad.Length)	ΔE (Mev)	$\frac{\sigma(with\ pre-radiator)}{\sigma(without\ pre-radiator)}$
1.0	0.7	30	1.0
1.0	1.7	130	1.2
3.0	0.7	40	1.0
3.0	1.7	180	1.1

Note: ΔE is the average shift of the energy with pre-radiator.

6. Radiative damage of lead glass counters in the Photon 3 detector.

6.1. Characteristics of lead glass counters in the process of irradiation.

The study of the radiative damage for different types of lead glass Cherenkov counters in γ spectrometers was performed on different beams of high energy particles in [8]. The measurements were done with counters from TF1-00, F8-00 and TF101 (radiative resistant lead glass) with dimensions $38 \times 38 \times 450$ mm^3, working with phototubes FEU-84.

The transparency of the counter is definited as

$$R = A_i/A_o, \tag{2}$$

where A_o and A_i are the phototube responses before and after irradiation. Transparencies R were measured with yellow and green LEDs and with the signals from electrons and muons (for lead glass counters irradiated in pion beam). The transparency depends on the flux of particles N, passing through the counter

$$R = exp[-N/b]. \tag{3}$$

The value of the slope $1/b$ depends on different circumstances: flash spectrum, photocathode spectral characteristics, energy of particles, $\sigma(abs)$ cross section of the particles.

In experiment of Ref.[8] it was obtained, that $b(yel.LED) > b(greenLED) > b(electron)$ (measurements were made after the irradiation in pion beam with E_π = 30 GeV).

It was approximated in [8], that

$$1/b \simeq const \cdot \sigma_{(abs)} \cdot E \tag{4}$$

Thus, for the lead glass T8 it was found that

$$\begin{aligned} b[\text{yel.LED; protons 70 GeV}]/b[\text{yel.LED; pions 30 GeV}] &\simeq 3.1(\text{experiment}); \\ &\simeq 2.9(\text{calculations with (4)}). \end{aligned} \tag{5}$$

But it must be stressed, that approximation (4), which is very important for our calculations for large energies, is not tested in the wide interval of E.

The final results of measurements [8] are presented in Table 2.

Table 2.

Glass type	b_e, 30 GeVπ^-	N_π for 80% residual transparency	
		E_π=30 GeV	E_π=600 GeV (est. with (4))
$F8$	$(7 \pm 2) \times 10^{10}$	1.4×10^{10}	7×10^8
$TF1$	$(5 \pm 1) \times 10^{10}$	1.0×10^{10}	5×10^8
$TF101$	$(4 \pm 1) \times 10^{12}$	8.0×10^{11}	4×10^{10}

6.2. The irradiation of Photon-3 detector in the hyperon beam with momentum $P_\Sigma \simeq 650$ GeV/c

The first analysis of the radiative damage in the lead glass counters in Photon-3 was made in [9]. But this analysis must be revised because new calculations are now available for the modified hyperon beam (with the enlarged collimator) and $\Sigma^- \rightarrow n\pi^-$ decay product distribution (Ref.[10] and Fig.8-11). Another factor is a new schedule with the $\sim$ 50-week run (old calculations were made for 16-week run).

When calculating the irradiation damage we really distinguish four kinds of fluxes causing different "slope" parameters b_i in the expression for transparency of irradiated lead glass counters

$$R_i = exp(-N_i/b_i).$$

The total transparency coefficient R is a product of all R_i

$$R = R_1 \cdot R_2 \cdot R_3 \cdot R_4,$$

where

R_1 relates to the Σ^--beam of 650 GeV energy;

R_2 relates to the π^--beam of the same energy;

R_3 is relevant to the π^- flux produced in $\Sigma \rightarrow \pi^- + n$ decay;

R_4 is relevant to the neutron flux from $\Sigma^- \rightarrow n + \pi^-$ decay.

As it have been discussed earlier (see expression (4)) the slope parameter b_1 depends on the energy and absorption cross section of particular fluxe. The Σ^- and π^- beam energies are fixed at 650 GeV, while the secondary π^- and n-fluxes have the energy spread. For example, the secondary π^- energy spectrum ranges from 120 to 170 GeV with the average energy of $\bar{E}(\pi^-) \approx$150 GeV. The secondary neutron energy spectrum spreads over the region 450-540 GeV with the average energy of $\bar{E}(n)$=500 GeV. So in the following calculation of b_i we use the average energies for secondary π^- and neutron-fluxes.

Thus for the transparency calculations we used the "effective neutron flux" and $[1/b_n]$ slope

$$N_{eff} = [N_n + (N_{beam}/1.27) + (N_\pi(\Sigma)/5.48)] \tag{6}$$

and

$$R = exp[-N_{eff}/b_n] \tag{7}$$

The resulting effective fluxes for different counters for 50 weeks of running are presented in Fig.12. The main radiation damage in neutral direction and around is caused by neutron flux. The decay π^- particles swept out to the right side of a beam (if you look downstream) produce the major radiation damage on that side. From these data it is possible to conclude that in order to reduce the radiative damage we must use in the Photon-3 practically all of our TF101 radiative resistant counters.

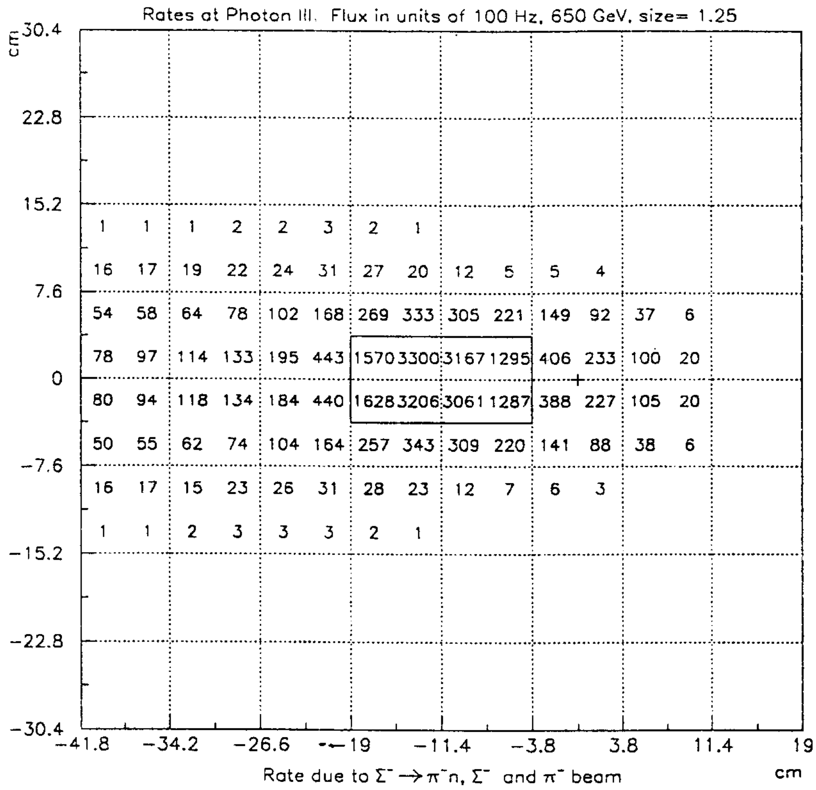

Fig. 8. **Rates in the Photon-3 detector for the beam with momentum of 650 GeV/c (collimator size 1.25) – total rates due to $\Sigma^- \to n\pi$; Σ^- and π^- beams in units of 100 Hz [10]. The proposed rectangular beam hole (2×4 counters) is marked by solid line.**

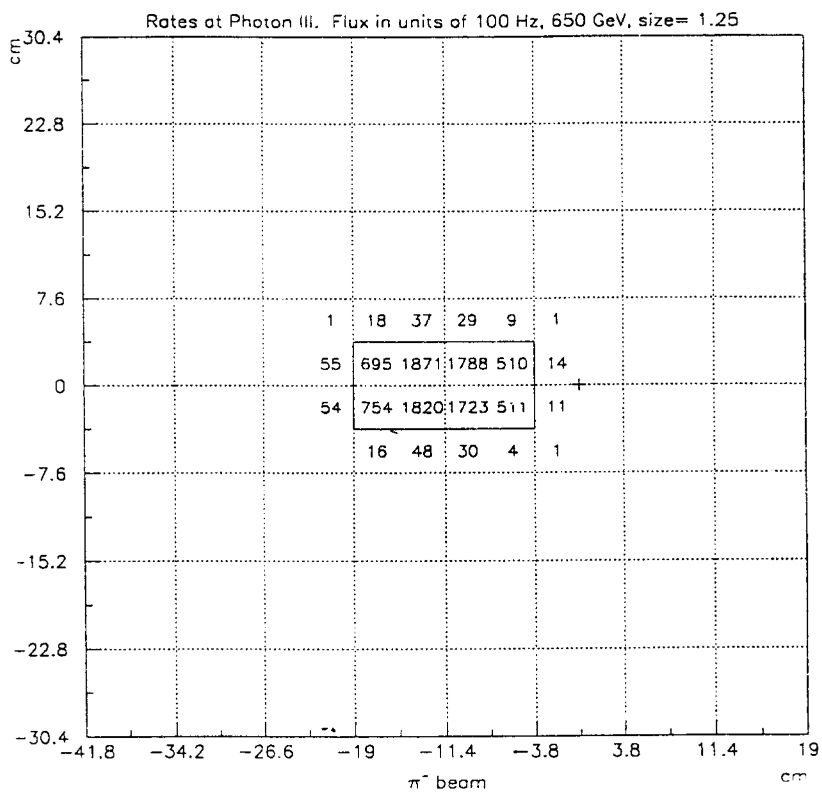

Fig. 9. The same rates, as in Fig.8, but only for the beam particles [10].

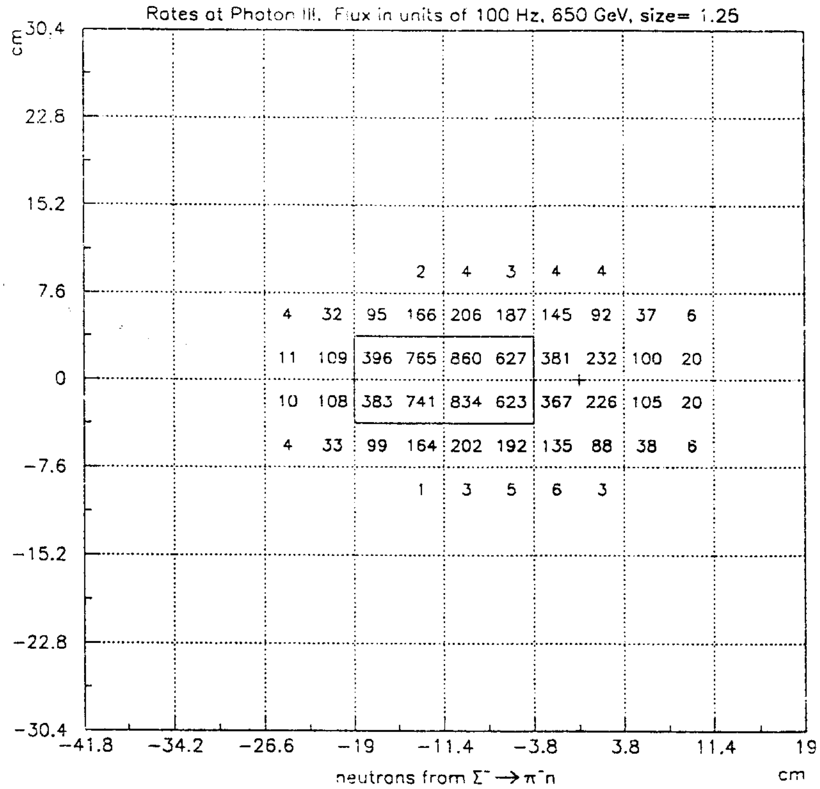

Fig. 10. The same rates, as in Fig.8, but only for neutrons from $\Sigma^- \to \pi^- + n$ [10].

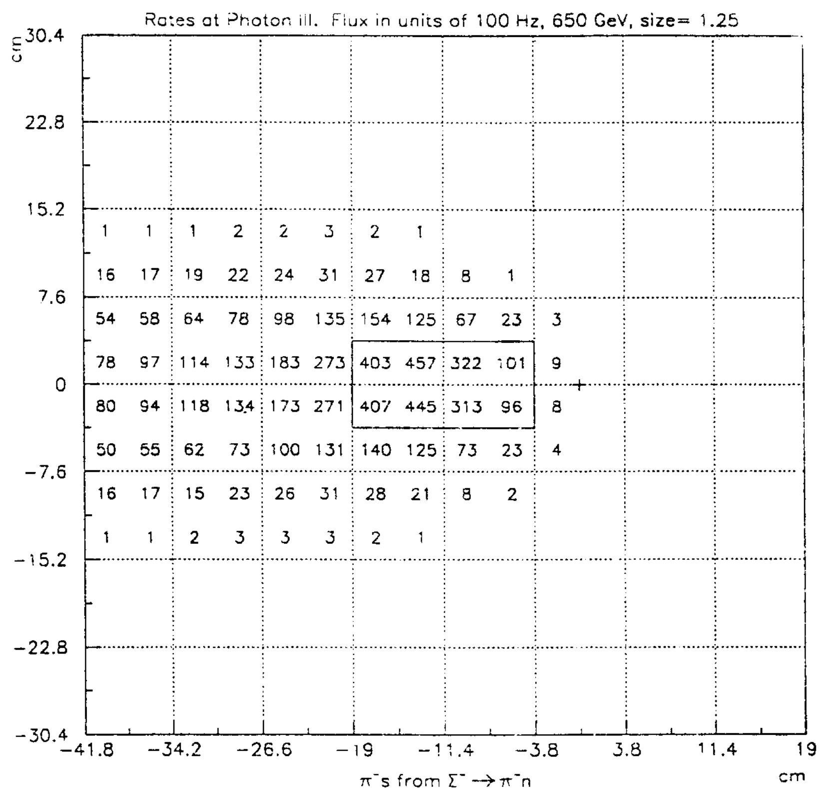

Fig. 11. The same rates, as in Fig.8, but only for pions from $\Sigma^- \to \pi^- + n$.

0,86 $\times 10^8$	1,3 $\times 10^8$	2,1 $\times 10^8$	2,1 $\times 10^8$	2,6 $\times 10^8$	1,7 $\times 10^8$	0,86 $\times 10^8$	< 7 $\times 10^7$							
0,15 $\times 10^{10}$	0,15 $\times 10^{10}$	0,19 $\times 10^{10}$	0,21 $\times 10^{10}$	0,27 $\times 10^{10}$	0,24 $\times 10^{10}$	0,26 $\times 10^{10}$	0,26 $\times 10^{10}$	0,21 $\times 10^{10}$	0,24 $\times 10^{10}$	0,16 $\times 10^{10}$	< 5 $\times 10^8$			
0,48 $\times 10^{10}$	0.54 $\times 10^{10}$	0,65 $\times 10^{10}$	1,0 $\times 10^{10}$	2.7 $\times 10^{10}$	6,5 $\times 10^{10}$	11 $\times 10^{10}$	11 $\times 10^{10}$	9,4 $\times 10^{10}$	6,6 $\times 10^{10}$	4.2 $\times 10^{10}$	2,4 $\times 10^{10}$	0,28 $\times 10^{10}$	< 5 $\times 10^{10}$	
0.82 $\times 10^{10}$	1,0 $\times 10^{10}$	1,2 $\times 10^{10}$	1,6 $\times 10^{10}$	9,8 $\times 10^{10}$	$\otimes$	$\otimes$	$\otimes$	$\otimes$	18 $\times 10^{10}$	11 $\times 10^{10}$ +	4,8 $\times 10^{10}$	1,0 $\times 10^{10}$	< 5 $\times 10^{10}$	

Fig. 12. The effective fluxes B_{eff} (see (6) and Table 3) in the counters of the Photon-3 detector for the run with a duration of 50 calendar weeks. The cross indicates the position of the neutral particle direction (12.6 cm from the middle of the beam hole). The beam hole is marked as $\boxed{\otimes}$. Only upper half of the Photon-3 detector is presented in this figure (because of the vertical symmetry).

Table 3. The evaluation of effective fluxes of particles in the counters (Fig.12)

	$P_{\text{beam}} = 650$ GeV/c			500 GeV/c
	TF101	TF1		
b_π(beam)	$1.85 \cdot 10^{11}$	$2.32 \cdot 10^9$	$b_\pi(\text{beam})/b_n = 1.27$	×1.3
$b_\pi(\Sigma^- \to \pi^- n)$	$8.0 \cdot 10^{11}$	$10.0^{.9}$	$b_\pi(\Sigma)/b_n = 5.48$	
$b_n(\Sigma^- \to \pi^- n)$	$1.46 \cdot 10^{11}$	$1.83 \cdot 10^9$		
	$\left.\begin{array}{r}\langle E_\pi\rangle = 500\text{GeV} \\ \langle E_\pi\rangle_\Sigma = 150\text{GeV} \\ \langle E_\pi\rangle_{\text{beam}} = 650\text{GeV}\end{array}\right\}$ data, for b_π(beam), $b_\pi(\Sigma)$, $b_n(\Sigma)$ obtained from Table 2 with the help of (4)			
$R = exp\{-(N_n/b_n) - (N_{\pi(\text{beam})}/b_{\pi(\text{beam})} - [N_{\pi(\Sigma)}/b_{\pi(\Sigma)}]\} = exp\{-N_{\text{eff}}/b_n\}$				
$$\begin{aligned} N_{\text{eff}} &= N_n + [N_{\pi(\text{beam})}/\frac{b_{\pi(\text{beam})}}{b_n}] + [N_{\pi(\Sigma)}/\frac{b_{\pi(\Sigma)}}{b_n}] = \\ &= N_n + [N_{\pi(\text{beam})}/1.27] + [N_{\pi(\Sigma)}/5.48] \end{aligned}$$				
To obtain the values for $N_{\pi(\text{beam})}$, $N_{\pi(\Sigma)}$, N_n we must use the rates in Figs.8-11, and to multiply these rates by the factor $F = 4.3 \cdot 10^6$ sec. Here $F =$ (50 weeks) $\cdot$ (83 hour/week)(1000 sec/hour) $= 4.3 \cdot 10^6$ sec - effective duration of 50 calendar weeks.				

6.3. New scheme for the Photon-3

In Fig.13 a new scheme of the Photon-3 detector is shown and the regions with TF101 and TF1 lead glass counters are marked. The transparences of the counters after 50 weeks of exposition are presented in Fig.14. It must be pointed out here again that the data in this figure have been obtained as a result of approximation (4), and this energy dependence of radiative damage needs further tests.

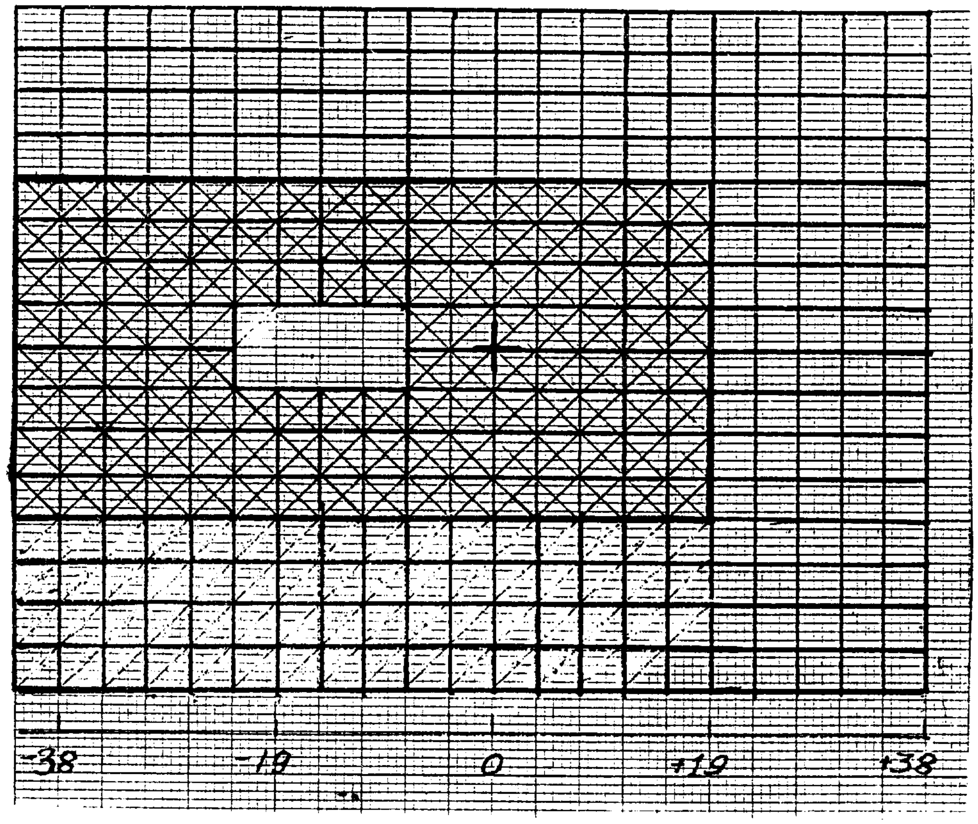

Fig. 13. Proposed arrangement of the radiative resistant counters from TF 101 lead glass in the Photon-3 detector.

As is clear from Fig.14, there is "dangerouse zone" in the Photon-3 detector (in spite of a rather large hole for the beam), in which the change of transparences of the counters during the run would be significant (more than by factor of 2). Thus for this "dangerouse zone" we need careful continuous calibrations during the run (using the laser, LED's, periodical calibrations of several counters in electron beam).

The influence of radiative damages on the resolution of γ spectrometer was studied in [8] for the spectrometer with TF1 lead glass. It can be presented in the form

$$[\sigma E/E] = [1 + \frac{10}{E^{1/2}} + 10 ln^2 R + \frac{30R}{E}]^{1/2} \cdot 10^{-2}, \tag{8}$$

and is illustrated by Fig.15. The coordinate reconstruction accuracy is less sensitive to a decrease of the radiator transparency. This accuracy is dependent mainly on the gradient of transparency. In the GAMS measurements this reduction in σ_y is several times less than σ_y even at $R = 0.15(\sigma_y \simeq 1.3$ mm at $E_e = 25$ GeV).

1,0,	1,0	1,0	1,0	1,0	1,0,	1,0	1								
0,99	0,99	0,99	0,99	0,98	0,98	0,98	0,98	0,98	0.98	0,99	1				
0,97	0,96	0,96	0,93	0,83	0,64	0,48	0,46	0,53	0,64	0,75	0,85	0,98	1		
0,95	0,93	0,92	0,90	0,51	⊗	⊗	⊗	⊗	0.29	0,48	0,72	0,94	1		

Fig. 14. **Transparencies R of counters in the Photon-3 detector after the irradiation with the effective fluxes of Fig.12.**

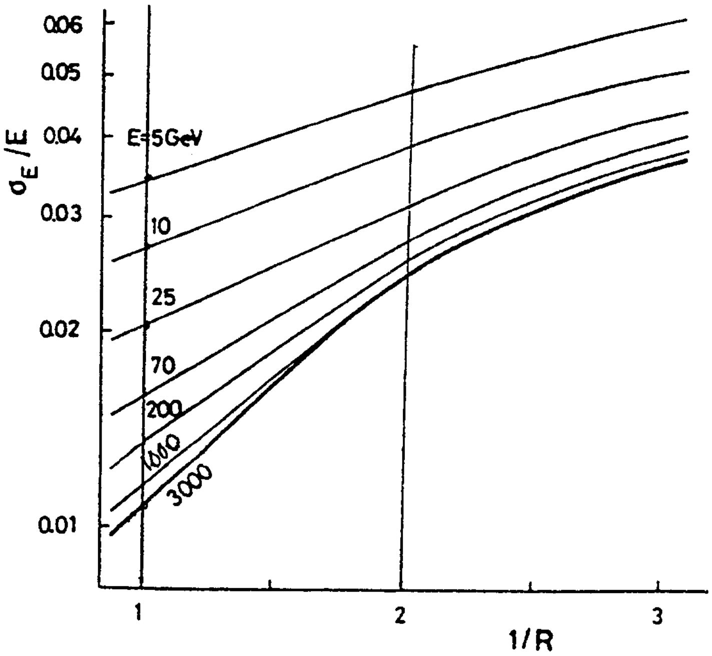

Fig. 15. Dependence of energy resolution on radiator transparency R for a spectrometer with TF1 lead glass counters [8]. The curves are expressions (8) in the text.

The Photon-3 detector must be used in a trigger of the second level for Primakoff production experiments (or may be in a part of them, connected with the polarizability measurements). Thus, to have a possibility to adjust the amplitudes of signals from a phototube when the transparency of the counter is changed during the run, we propose to have an individual regulation of HV on ~ 50 counters in the "dangerous zone". These counters with the individual HV control are shown in Fig.16.

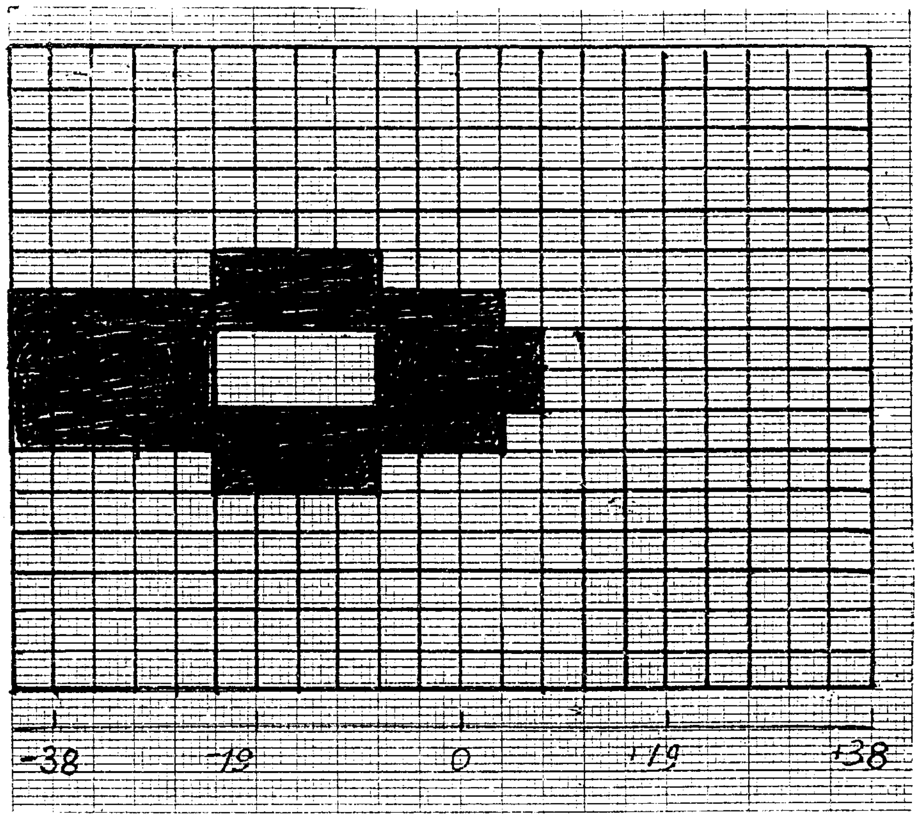

Fig. 16. Proposed arrangement of the counters with individual HV control in the Photon-3 detector (the blackened area).

It is possible, that in the two intervals between main parts of the run we should revise the Photon-3 for the recovering of the transparency of some counters. Because of lack of spare counters with TF101 radiative resistant glass, the technique of UV irradiation for the recovering from the radiative damage [11] must be used in this case. This technique is under study now.

7. Conclusion

Our general conclusion: with the present geometry and the beam intensity the Photon-4 detector is almost useless for the measurements of high energy γ's.

We think that the best way out is to use only one detector (the Photon-3), fully equipped with radiative-resistant lead glass blocks and high voltage channels from the Photon-4. In this case the Photon-3 will measure the energy and coordinates of γ's for the energies up to 200 GeV and coodrinates only for higher energies, where for specific reactions the beam constrained method would be used for E_γ measurements.

We would like to thank Yu.Prokoshkin, and also D.Casey, P.Cooper, T.Ferbel, J.Russ, A.Szijmulanski, Z.H.Zhu and other members of E781 Collaboration for helpful discussions.

References

[1] Edelstein R. et al. – Fermilab Proposal E781 (1987) (revised July, 1993).

[2] Lach J., Gottschalk E. – H-460 R7 (E781 Layout), September 1994.

[3] Adams D.L. et al. – Preprint IHEP 91-100, Protvino, 1991.

[4] Zhu Z.H. – E781 H-notes 650 (October, 1993) and 651(November, 1993).

[5] Aronson S. et al.//NIM, A269 (1988) 492.

[6] EGS Monte-Carlo. – SLAC-PUB-4649 May, 1988.

[7] Brabson B.B. et al. – BNL Preprint BNL, 1993.

[8] Inyakin A.V. et al.// NIM, 215 (1983) 103.

[9] Landsberg L.G. – E781 H-hote 641 (September, 1993).

[10] Casey D., Ejnisman R. – E781 H-note 686 (May 1994).

[11] Kobayashi H. et al. – Preprint IHEP 94-8, Protvino, 1994 (in Russian).

Received July 21, 1995

Appendix 1

Table 4. Chemical structure of lead glass.

	TF1-000	TF101
Pb0	51.2%	51.23%
SiO_2	41.3%	41.53%
K_2O	7.0%	41.53%
As_2O_3	0.5%	-
CeO_2	-	0.2%
Density (g/cm^3) – 3.86		
Radiation length (cm) – 2.8		
Refractive index, n_e – 1.6522		

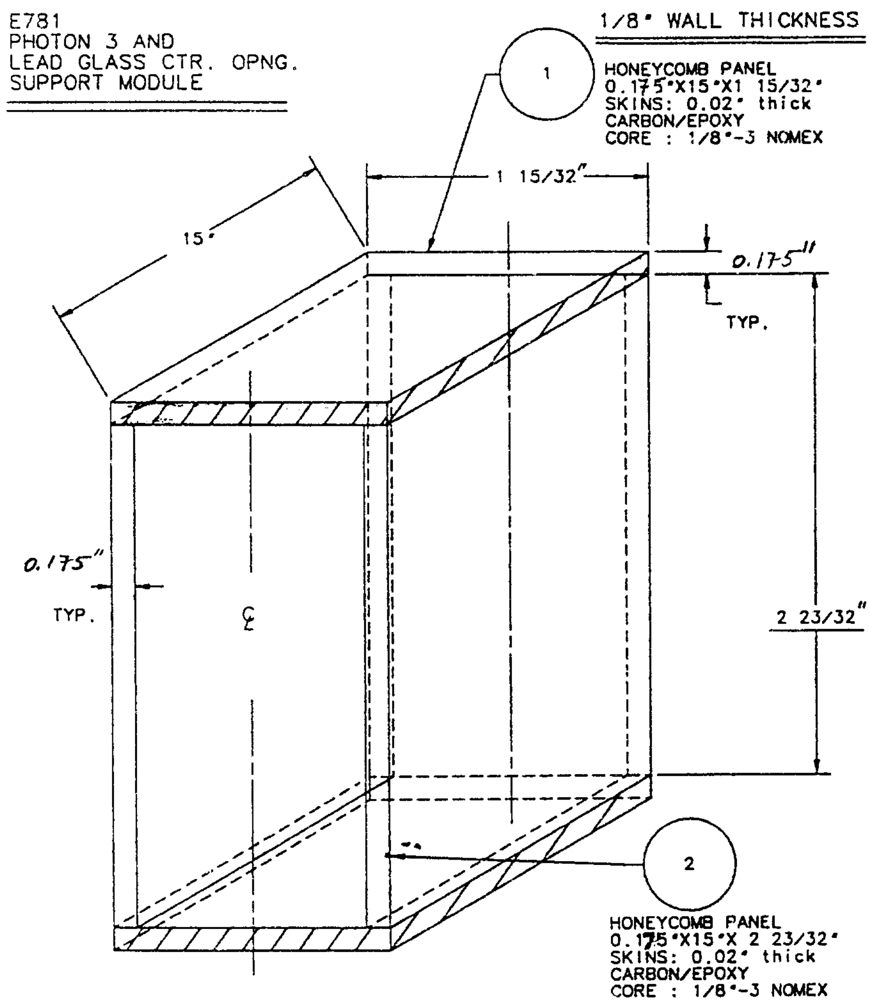

Fig. 17.

Appendix 2

Instead of 8 lead glass counters taken off in order to make a hole for beam particle the 4-support modules have been installed. The dimension of one of 4 modules are shown in Fig.17. They are made from PN Aramid Honeycomb material having the following features:

- high strength to weight ratio;
- corrosion-proof;
- good thermal insulation;
- fire-proof (self-extinguishing);
- easily shaped;
- excellent dielectric properties;
- very bondable.

The PN Designates Aramid Fiber Honeycomb has the density (in pounds per cubic feet) ρ=0.3. Besides the fitting to the hole sizes the support modules must meet the following requirements:

to be strong enough to support seven lead glass counters ($\simeq$20 kg) supported by each module;

to absorb a small fraction of the beam.

As each module has two supporting planes (side planes, front and rear parts are open) the strength of these planes is equal to 40 kg in the worst case. Therefore there is a safety factor of the order of two. The fraction of absorbed (by nuclear interaction) beam assuming that the $\lambda_{in}(hooneycom) = \lambda_{in}(carbon)$=60.2 g/cm^2 is 3%, while for electromagnetic interaction the portion of the converted beam is 4.3%. Since only 24% of the beam is obstructed by honeycomb panel, the loss of beam will be smaller by an additional factor of 4.

Ю.М.Гончаренко и др.
Фотонный детектор для измерений при высоких энергиях для спектрометра SELEX (эксперимент E781, Fermilab).

Оригинал-макет подготовлен с помощью системы LaTeX.
Редактор Е.Н.Горина. Технический редактор Н.В.Орлова.

Подписано к печати 07.08.95. Формат 60 × 84/8. Офсетная печать.
Печ.л. 2,75. Уч.-изд.л. 2,1. Тираж 240. Заказ 464. Индекс 3649.
ЛР №020498 06.04.92.

ГНЦ РФ Институт физики высоких энергий
142284, Протвино Московской обл.

Индекс 3649

П Р Е П Р И Н Т 95-109, И Ф В Э, 1995